RESEARCH ARTICLE

Characterizing bedforms in shallow seas as an integrative predictor of seafloor stability and the occurrence of macrozoobenthic species

Kasper J. Meijer[1] (iD), Oscar Franken[1,2] (iD), Tjisse van der Heide[1,2], Sander J. Holthuijsen[2] (iD), Wim Visser[3], Laura L. Govers[1,2] (iD) & Han Olff[1] (iD)

[1]Conservation Ecology Group, Groningen Institute for Evolutionary Life Sciences (GELIFES), University of Groningen, P.O. Box 11103, 9700 CC, Groningen, The Netherlands
[2]NIOZ Royal Netherlands Institute for Sea Research, Department of Coastal Systems, P.O. Box 59, 1790 AB, Den Burg, Texel, The Netherlands
[3]Rijkswaterstaat Centrale Informatievoorziening, P.O. Box 2232, 3500 GE, Utrecht, The Netherlands

Abstract

In soft-bottom marine ecosystems, bedform variation is induced by wind- and tidal-driven hydrodynamics. The resulting megaripples, sand waves and sandbanks form a spatially and temporally heterogeneous seafloor landscape. The strong physical forces imposed by the migration of these bedforms are important determinants for the occurrence of different macrozoobenthic species. Quantifying the effect of these forces can help in differentiating natural- and anthropogenically induced physical stressors. However, large-scale mapping of seabed morphology at high resolution using multibeam echosounder is challenging, costly and time-consuming, especially in shallow seas, prohibiting wide swaths. Instead, their bathymetry is typically studied using single-beam transects that are interpolated to bathymetric grids with a relatively coarse resolution (20 m). However, this leaves out information on smaller scale (<20 m) bedforms that can be ecologically relevant. In the Dutch Wadden sea, a shallow tidal system, we characterized bedform variation at high resolution using single-beam data for the first time. We calculated a 2-D Terrain Ruggedness Index (TRI) at sub-meter resolution along the single-beam transects and interpolated the results to a full 3-D grid. We then validated the result by relating TRI to independently modeled hydrodynamic parameters and to the distribution of macrozoobenthic species. We found that TRI successfully integrates the variation of tidal-driven bed shear stress and wave-driven orbital velocity. In addition, we found TRI to be a good predictor of the occurrence of macrozoobenthic species. The inferred small-scale bedforms provide valuable information for separating the relative importance of natural dynamics *versus* anthropogenic disturbances such as dredging and bottom trawling activities. We discuss that by repurposing already available single-beam data in this way, bedforms can be characterized at high resolution without the need for additional equipment or mapping campaigns, yielding novel input to decision-making on marine management and conservation.

Introduction

Coastal morphodynamics studies the complex interplay between hydrological properties, seafloor dynamics and biological and anthropogenic processes in the coastal zone (Wang et al., 2012). Coastal ecosystems are dynamic and diverse systems of large ecological and societal importance (Barbier et al., 2011; Costanza et al., 1997) and are among the densest populated areas worldwide, resulting in extensive exposure to anthropogenic stressors (Harley et al., 2006; He & Silliman, 2019). In soft-bottom ecosystems, benthic marine macrofauna are important determinants of marine biodiversity and a range of ecosystem services (Snelgrove, 1999). In these systems, the relative

importance of natural dynamics *versus* negative additional impacts of bottom trawling fisheries, dredging for shipping and sand supplements for coastal protection on biodiversity and ecosystem functioning have been the subject of much debate (Pitcher et al., 2022; Rippen et al., 2021; van Dalfsen et al., 2000). Anthropogenic disturbances on top of natural dynamics may significantly alter benthic communities. Mapping the key natural environmental determinants of macrobenthic communities is therefore important in understanding the status and restoration potential of these ecosystems, contributing to sustainable marine spatial planning. This requires a clear separation of anthropogenic and natural determinants of biodiversity and ecosystem functioning.

Species distributions are strongly linked to underlying abiotic conditions. The potential occurrence of a species is dependent on their response traits in relation to the possible physiological conditions they can withstand (Kraft et al., 2015). On a large spatial scale, it is generally accepted that with increasing depth, differences in light, temperature and salinity are important physiological constraints for the occurrence of benthic species (Snelgrove, 1999). However, on a more local scale, variation in hydrodynamic conditions and sediment dynamics are an additional important determinant of species distributions (de Jong et al., 2015; Rosenberg, 1995; van der Wal, Lambert, et al., 2017a). In shallow near-shore zones of soft-bottom systems, differences in hydrodynamic conditions lead to variation in seabed morphology through a combination of near-bed flow processes, wave-driven orbital velocities and sediment sorting and transport (Barman et al., 2016; Dodd et al., 2003; Morales et al., 2015).

Different bedforms thus reflect variation in natural hydrodynamic conditions and in the nature and intensity of sediment transport (Barnard et al., 2011; Lefebvre et al., 2016). Bedforms in turn impose strong selective forces on their associated fauna as with fast moving bedforms, species have to deal with strong variation in burial and exposure (van der Wal, Ysebaert, et al., 2017b). Migration rates of regular bedforms are dependent on their wavelengths (Ernstsen et al., 2005; Wever, 2004) which are highly correlated with wave height (Flemming, 1988). Different sized bedforms thus migrate at different speeds, resulting in different temporal- and spatial scales of ecological impact (Fig. 1). Small bedform patterns, such as sand ripples can move at rates of several meters per hour (Knaapen, 2005). However, the small wave heights of several centimeters make their burial effect negligible leading to low ecological impact. In contrast, large-scale bedform patterns, such as sandbanks and sand waves can reach heights of several to tens of meters (Knaapen, 2005). Nevertheless, their migration rates are only several meters per year, timescales that macrobenthic communities can more easily adapt to. Intermediate bedforms, such as megaripples with wave heights of generally half a meter, are known to move with several meters per day up to a meter per hour (Brakenhoff, 2021; Knaapen, 2005). For macrozoobenthic species, this would mean burial of several decimeters of sediment for hours up to days at a time. Considering that epifaunal suspension feeders and large deep-burrowing siphonate suspension feeders are generally not able to adapt to more than 1 cm of burial due to a restricted mobility (Kranz, 1974), these kinds of burial dynamics have the largest
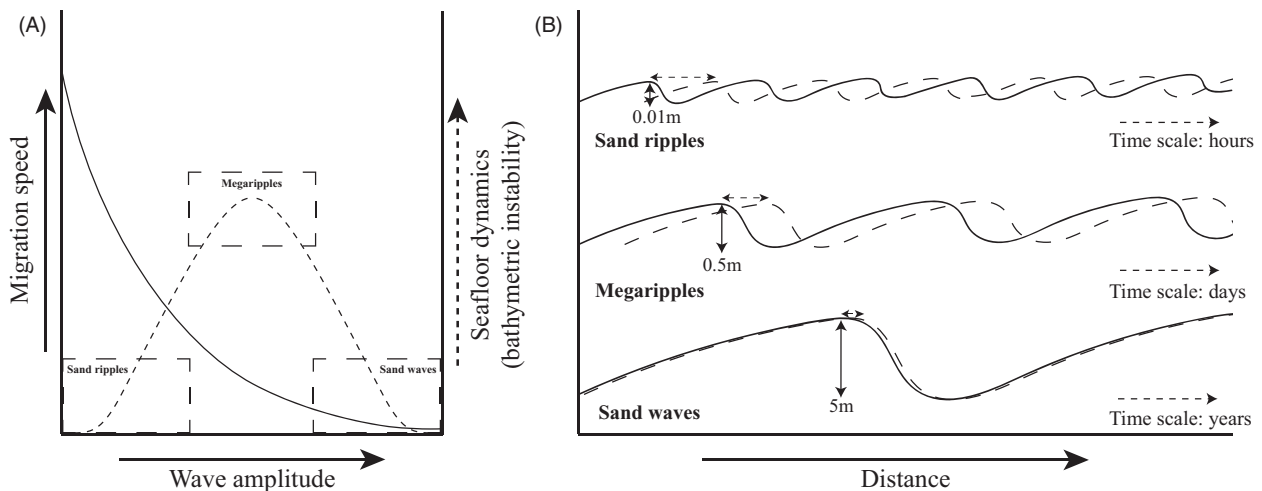

Figure 1. Visualization of (A) the impact of seafloor dynamics in relation to wave size and migration speed; and (B) bedform migration in relation to their scale. Small bedforms migrate faster but their vertical sediment displacement is also lower. Larger bedforms have significant sediment displacement throughout one wave period but move at such slow rates that communities can easily shift along. Ecological impact through seafloor dynamics is thus highest at intermediate-sized bedforms (*i.e.*, megaripples). Based on Knaapen (2005).

consequences for associated macrozoobenthic fauna. Highly dynamic environments are then generally dominated by mobile and short living, resistant and/or resilient species, while low dynamic environments are often characterized by sessile, long living species that are more vulnerable to disturbances and are generally low-resilient (Holzhauer et al., 2022). By mapping small-scale bedform variation, we can identify areas that are potentially highly diverse and vulnerable systems based on underlying natural dynamics and prioritize these areas for conservation.

For offshore soft-bottom systems, the relation between bedform variation and macrobenthic communities is relatively well studied (*e.g.* Baptist et al., 2006; Damveld et al., 2018; Markert et al., 2015). Some studies indeed show that bedform variation may explain important variation in macrobenthic species distribution in near-shore systems as well (Holzhauer et al., 2019, 2022; van der Wal, Ysebaert, et al., 2017b), but seascape-wide mapping studies are still lacking, especially for the more shallow parts of soft-bottom coastal systems. While the seafloor of deeper parts of coastal shelves and seas is often mapped using multibeam echosounders, this technique is more challenging to apply in more shallow estuaries and barrier island inlet lagoons, as the obtained swath width is limited by the depth, making the mapping of large areas expensive (Landero Figueroa et al., 2021). Single-beam echosounding is a cheaper method for mapping bathymetry but has a smaller coverage and is usually interpolated to larger areas at coarser resolution. For example, single-beam data have been used to create bathymetric maps of the entire Dutch subtidal Wadden Sea every 6 years at 20 m grid cell resolution. However, small bedforms of high ecological relevance, such as megaripples, are not represented during gridding and interpolation of these extensive mapping surveys (Brakenhoff, 2021), complicating the assessment of the relationship between natural bedform occurrence and macrozoobenthic communities. Hence, we aim to (1) determine small-scale bedform variability by calculating a Terrain Ruggedness Index (TRI) based on single-beam survey data and interpolating this to the whole landscape, (2) check if this TRI reflects temporal dynamics by relating it to historic bathymetry data and (3) relate high-resolution bedform data to macrozoobenthic species. For this, we analyzed and combined a single-beam and benthic species survey dataset from the Western Dutch Wadden Sea.

Material and Methods

Study area

The Wadden Sea is one of the largest intertidal ecosystems in the world and consists of 33 tidal inlet systems along the Dutch, German and Danish coast (Lotze et al., 2005; Reise, 2005). Barrier islands separate the North Sea from the intertidal flats that are divided up into tidal basins (Elias, 2006). For this study, we focused on the Marsdiep tidal basin in the Western part of the Dutch Wadden Sea (Fig. 2). This is the largest tidal basin (690 km^2) of the Dutch Wadden sea (Oost et al., 2018)
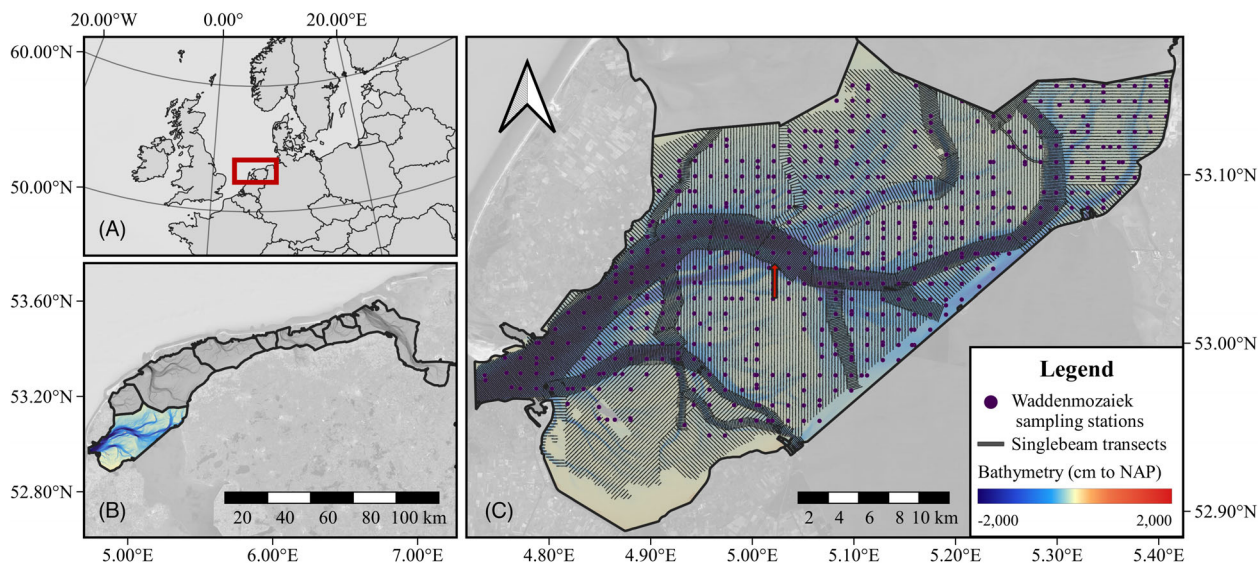

Figure 2. Map of study area. (A) Map showing north-west Europe, highlighting the Dutch Wadden Sea in red. (B) Zoomed in area of the Dutch Wadden Sea, the colored tidal basin indicates the Marsdiep tidal basin. (C) The Marsdiep tidal basin study area with underlying bathymetric map. Bathymetry is shown in cm to NAP (Amsterdam Ordnance Datum). Black lines depict the single-beam echosounding transects and the dots indicate the location of benthos samples collected in 2019. The red arrow depicts the transect shown in Figure 4.

and is the most western tidal basin situated between the island of Texel and the provinces Noord-Holland and Friesland (Fig. 2).

Terrain ruggedness index calculation

The Terrain Ruggedness Index (TRI) is a measure for terrain variability that can be calculated from bathymetric data (Wilson et al., 2007). TRI is a measure of the variability of depth around a central pixel and is calculated as the average absolute difference of the central pixel with each of its neighbors for a particular window size (Wilson et al., 2007). It is a focal statistics measure, meaning that windows applied to neighboring pixels are overlapping while the original resolution of the data is retained. Here, TRI was derived from the raw single-beam echosounder data also used for the interpolation of the bathymetric map for 2015 by Rijkswaterstaat (Fig. 2) (de Kruif, 2001). To accomplish this, the single-beam data was first rasterized to gridded line transects at 1 m resolution, as done before for the bathymetric interpolation (van Prooijen et al., 2020). For each raster cell, the TRI was calculated using a 55 meter window size with the "tri" function in the spatialEco package (Evans et al., 2021) in R-Studio, R-version 4.1.0. (R Core Team, 2021). Megaripples, a mesoscale bedform in current-dominated conditions (Hulscher, 1996) - that is larger scale than sand ripples but smaller than sand waves - have typical wavelengths between 0.6–20 m (Idier et al., 2004), but wave lengths of up to 28 meters have been measured for the Ameland tidal inlet in the Wadden Sea (Brakenhoff, 2021). The single-beam transects likely do not run from crest to trough of each megaripple, as the transects are perpendicular to the direction of the main gulley. Still, the megaripples are not uniform in shape and crests do not line up perfectly parallel. The transects therefore do cross crests and troughs of different ripples but with likely larger wavelengths than 28 meter. By taking a window size of 55 m around a focal pixel, we ensure that at least one entire megaripple can potentially be included in the calculation. To discern the effects of the transects not running perpendicular to the megaripple wave direction, single-beam transects were simulated on available multibeam data for the Marsdiep inlet. For this simulation, the transects were created to run perpendicular to the megaripple formations and parallel to the main gulley (Appendix A). The TRI calculation results in a raster containing 100–200 m spaced transects of equal configuration to the original single-beam echosounder dataset (Fig. 2c). These transects now contained a value of TRI (in m) instead of depth to mean sea level for each pixel, reflecting the mean of the absolute differences of all depths in that window to the mean depth of the window, both measured in meters. For example, a TRI of 5 implies for a focal pixel that all pixels within a 27 m radius ((55–1)/2) around it are on average 5 m higher or lower than that focal pixel. The obtained value was multiplied by 100 and natural log transformed to normalize the statistical distribution of the residuals when used in a regression. Because the result is still an index, this log(TRI*100) will be abbreviated as TRI from here onwards. This TRI value was interpolated to a seascape-covering grid at 20 m resolution using the same interpolation application (DIGIPOL) used for the Wadden Sea bathymetric maps. A 20 meter grid was chosen as this is also the standard grid size that is used for the regular bathymetric interpolation. Since the transects are 100–200 meters apart, a 20 m resolution gives the best mathematical approximation of the unknown bathymetry. DIGIPOL is an iterative linear interpolation method based on triangulation within the MARIA software package (Rijkswaterstaat, RIKZ, 2021). As high TRI values can indicate both small-scale variation in bedforms on large-scale flat seafloor surfaces, as well as steep slopes on edges of gullies (what we are not interested in here), we masked the map at locations with a slope in bathymetry higher than 65 degrees. Slope was derived from the original 20 m resolution bathymetry map using QGIS version 3.18.1 (QGIS Development Team, 2021). Slope and TRI were then compared in predictive power for the occurrences of species to highlight the added value of TRI as an indicator for natural dynamics. Masked areas are not taken into account for the analyses.

Abiotic data

Bathymetry

Bathymetric data has been collected since 1985 by the Ministry of Infrastructure and Water Management of the Netherlands (Dutch: Rijkswaterstaat) (de Kruif, 2001). For subtidal areas, this is done by combining single-beam echosounder (NAVISOUND 200) data collected at a resolution of approximately 30 cm along transects spaced approximately 200 meters apart (Fig. 2c). Lidar data of 1 m resolution is used for the intertidal flats. These combined data were interpolated to a 20 m resolution grid (van Prooijen et al., 2020). The echosounding was typically done in relatively calm weather conditions, which may underestimate bedform heterogeneity during stormy conditions. Hence, the obtained TRI values are probably a conservative estimate, and observed patterns might be stronger under more severe weather conditions. On the other hand, bedform patterns may be strongly modified (higher or lower amplitude, different phase and direction)

by stormy conditions and then the obtained TRI could be an overestimation. Nevertheless, macrofauna still have to cope with these severe sediment dynamics.

Bathymetric instability

We used the 20 m resolution bathymetric maps derived with the previously described procedure as measured in the periods 1985–1989, 1990–1994, 1995–2000, 2001–2006, 2007–2013 and 2014–2020 to calculate the absolute mean annual changes in depth as an indicator for seabed stability. For the different years of observation, the absolute bathymetric difference was calculated for each period (t) with its consecutive period (t + 1). This difference was standardized to mean absolute depth change per pixel per year for each period by dividing it by the period length in years. Finally, the mean depth change per pixel per year over all periods was calculated (See Appendix B for further details).

Orbital velocity, flow rate and bed shear stress

We related variation in bedform and bathymetric stability to several modeled hydrodynamic variables. Orbital velocity was predicted using the SWAN-Kuststrook wave model using March 2020 wave measurements as a representative for average annual wave conditions (Van Weerdenburg & Vroom, 2021). The root mean square of the amplitude of the predicted orbital movement was interpolated to a 100 × 100 meter grid as representative value for orbital velocity (Van Weerdenburg & Vroom, 2021). Bed shear stress and flow rate were calculated using the Dutch Wadden Sea Model (DWSM) in the hydrodynamic model Delft3D-Flexible Mesh (Van Weerdenburg & Vroom, 2021). Bed shear stress and flow rate are based on a 2D version of the model and also interpolated toward a 100 × 100 meter grid (Van Weerdenburg & Vroom, 2021).

Sediment properties

A large-scale sampling campaign was conducted in 2019 throughout the subtidal Dutch Wadden Sea. In this campaign, sampling points were arranged in a 1 × 1 km grid with additional random points (Franken et al., n.d.). Points were sampled for sediment properties and benthic macrofauna. Deeper parts were sampled using a 20 x 30 cm boxcore (0.06 m^2). More shallow areas were visited using a Zodiac and four benthos cores (Ø 10.4 cm) were taken and combined at these locations (0.035 m^2). At each sampling location, a sediment sample was taken of the upper 4 cm and immediately frozen at −20°C. In the lab, the samples were subsequently freeze-dried for up to 96 h and then homogenized with a mortar and pestle. Prior to grain-size analysis between 0.5 and 5 grams, depending on the estimated grain size, of homogenized sample was weighed over a 2 mm sieve, in 13 mL PP Autosampler tubes. RO water was added and the sample was shaken vigorously on a vortex mixer for 30 s. Median particle size and the percentage silt (fraction <63 μm) of sediments were determined using a Coulter LS 13 320 particle size analyzer and Autosampler. The optical module "Gray" was used for the calculations (Compton et al., 2013). Median grain size (D50) and silt percentage per sample were used for further analysis.

Biotic data

We tested the predictability of TRI for the occurrence of macrobenthic species to see if TRI is a useful indicator of seabed stability and natural dynamics. The species data were also obtained from the sampling campaign in 2019. Macrobenthic samples were sieved over a 1 mm mesh in the field. Larger shellfish were kept separate and stored frozen. All other living organisms were stored on a pH-buffered 6% formaldehyde solution and stained with Rose Bengal (CAS Number: 4159-77-7) for sorting. In the lab, all individuals were identified to the lowest taxonomic level possible, in most cases to species level (Compton et al., 2013). We used presence–absence data of these species for further analysis.

Statistical analyses

TRI vs. abiotics

The relation between Terrain Ruggedness Index (TRI), as calculated in this study, and various bathymetric and hydrodynamic variables was explored by calculating the Pearson correlation coefficient between all factors using the "cor" function in base R. Prior to this, variables were checked for linear relationships. Bed shear stress, orbital velocity and bathymetry were ln(x + 1) transformed, and slope was square-root transformed to linearize their relationship with TRI. P-values were determined for these correlations using the "cor_pmat" function in the "ggcorrplot" package (Kassambara, 2019). Significant correlations were then plotted using the same package. Subsequently, these correlations were explored through multiple linear regression as well as additive models on the untransformed variables using the "mgcv" package (Wood, 2011). Predictor variables were first tested for collinearity by determining VIF scores (Variable Inflation Factors). Variables with VIF scores higher than 5 were sequentially removed until no collinearity could be

detected anymore (Alin, 2010). Flow rate and bathymetry had high multicollinearity with each other as well as with orbital velocity and bed shear stress. Flow rate and bathymetry had highest VIF scores and were therefore removed. In the final model, orbital velocity, median grain size (D50), percentage of silt and bed shear stress were used as predictor variables in a linear model. Additive models did not significantly enhance model predictions (Appendix C) and linear models were chosen for ease of interpretation. The model variables were tested for significance and model assumptions were checked. The best model was selected through stepwise backward selection.

Subsequently, the newly obtained TRI map was related to the bathymetric instability through a linear model. For this, the mean annual absolute bathymetric difference calculated over the last 40 years was $\ln(x + 1)$ transformed and used as a response variable in a linear model, checked for assumptions and significance.

TRI *vs.* species occurrences

To test if the TRI was related to macrozoobenthic species occurrence, we extracted the 20 m-interpolated value from the TRI raster at the geographic location of each benthos core sample. We used the presence–absence data of all identified taxonomic groups that were found in more than 10 samples. We then explored how their probability of occurrence depended on the TRI using generalized linear models with a binomial distribution, testing for a quadratic effect of TRI (reflecting an ecological optimum in probability of occurrence). For each species, the model was tested for overdispersion, in which case a quasibinomial distribution was used instead. From the set of predictor variables, the best model was chosen using stepwise backward selection (so retaining the linear term when the quadratic term was significant). Then, a weighted average of TRI (ecological optimum (Ter Braak & Prentice, 2004)) was calculated for all taxonomic groups that showed a significant relationship between TRI and the probability of occurrence. For this, the TRI value was averaged for all taxonomic groups over all sampling locations where this group was present. Finally, six species that showed low, intermediate and high weighted averages of TRI were further explored. This was done by plotting a regression line based on the significant binomial model determined above.

As mentioned before, high TRI values can indicate both small-scale variation in bedforms on large-scale flat seafloor surfaces, as well as steep slopes on edges of gullies. To show the added relevance of TRI compared with using slope, the same generalized linear models were used with slope as a predictor instead.

Results

TRI calculation

By interpolating the Terrain Ruggedness Index (TRI) values obtained from the single-beam transect data, we were able to create a map of the TRI values for the whole Marsdiep tidal basin (Fig. 3). Even after masking areas where TRI values were high due to the effect of steep slopes of gullies, we observed that TRI values were highest in the deeper gullies (Fig. 3; Appendix D). These patterns were also observed in the original single-beam transect, high-resolution data, where single-beam transects crossing deeper gullies showed larger small-scale variation in the deeper parts than in the shallower areas (Fig. 3). The 20-meter interpolated bathymetry map did not capture this small-scale bathymetric variation, which shows that the calculated TRI values presented in this paper were able to distinguish between small-scale bedforms that are typically not resolved when processing raw single-beam data to bathymetric maps (Fig. 4). Simulating transects that run perpendicular to the bedform migration does not result in major differences of TRI compared with the original transects either (Appendix A).

TRI in relation to hydrodynamic and bathymetric factors

We tested how the derived TRI values relate to other independently modeled and derived abiotic data. The correlogram of the Pearson correlation coefficient showed strong correlations between TRI and the hydrodynamic and bathymetric factors. There was a strong negative correlation between TRI and bathymetry (-0.72) as well as with orbital velocity (-0.75). On the other hand, TRI was strongly positively correlated with bed shear stress (0.76), current velocity (0.75) and slope (0.88). Median grain size was only weakly positively correlated with TRI (0.42), whereas median grain size was strongly positively correlated with bed shear stress (0.63) and current velocity (0.62). Hydrodynamics and bathymetry were likewise strongly correlated, indicating the strong codependence between all variables (Fig. 5a).

High TRI was related to a high mean annual change in bathymetry over the past 35 years ($B = 1.08$, 95% CI [0.95, 1.22]), as TRI and mean annual change in bathymetry ($\ln(x + 1)$ transformed) were positively correlated ($F_{(1,519)} = 261.76$, $p < 0.001$, $R^2_{adjusted} = 0.33$) (Fig. 5b).

TRI and bed shear stress were positively correlated ($F_{(1,518)} = 147.90$, $p < 0.001$) (Fig. 5c), whereas TRI and orbital velocity were negatively correlated ($F_{(1,518)} = 118.43$, $p < 0.001$) (Fig. 5d). Both bed shear stress and orbital velocity were strong predictors of
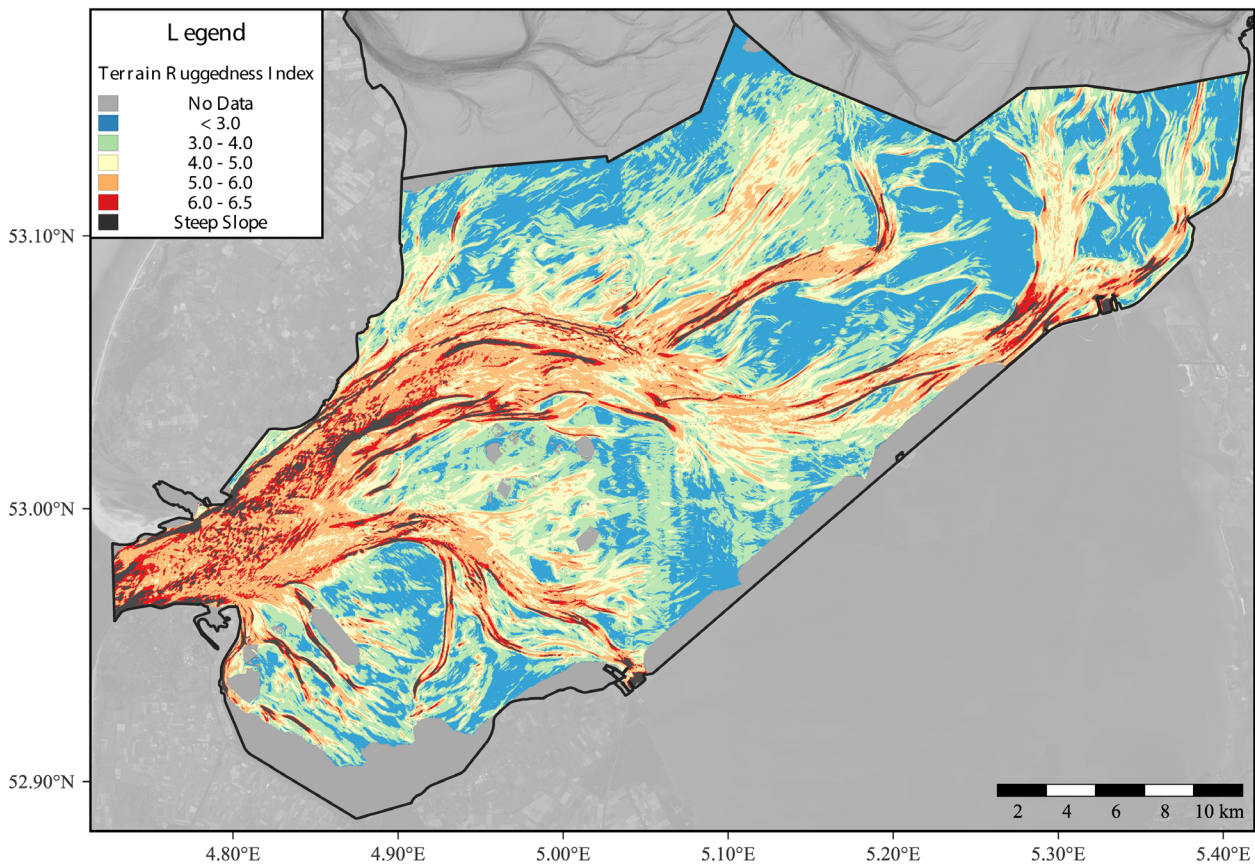
Figure 3. Map of the variation in Terrain Ruggedness Index (TRI) for the Marsdiep tidal basin interpolated from the transects in figures 1 to 20 m resolution. Colors represent TRI values. High TRI values caused by steep slopes (>65 degrees) have been masked out in dark gray.

TRI explaining up to two-thirds of the variations ($R^2_{adjusted}$ = 0.66, n = 518).

Median grain size was excluded from the model due to its strong relationship with bed shear stress (F $(1,519)$ = 337.16, $p < 0.001$, $R^2_{adjusted}$ = 0.39; Figure 5c; Appendix D) and orbital velocity (F $(1,519)$ = 94.35, $p < 0.001$, $R^2_{adjusted}$ = 0.15; Figure 5d; Appendix D). Nevertheless, median grain size shows a strong gradient along the TRI values (Fig. 5c; d).

TRI as an indicator for the occurrence of species

We found significant relationships between our TRI and the occurrence of 31 out of 50 tested taxa (Fig. 6; Table D2, logistic regressions). In the majority of cases, TRI was a better indicator in predicting the occurrence of taxa compared with slope (Appendix E), highlighting the added value of TRI in modeling species occurrence and habitat mapping. High TRI values were associated with mobile scavenger–predator species like *Nephtys cirrosa* and *Eumida sanguinea* (Fauchald, 1977; Hayward & Ryland, 2017) as well as

mobile deposit-feeding species, such as *Bathyporeia* spp. and *Microphthalmus* sp. (Fauchald, 1977; Nicolaisen & Kanneworff, 1969) (Fig. 6). *Bathyporeia* spp. and *N. cirrosa*, with high weighted averages of 4.38 and 5.13, respectively, showed an increase in occurrence with increasing TRI (binomial regression, B = 0.30, 95% CI = [0.13, 0.47] and B = 0.81, 95% CI = [0.41, 1.27], respectively; Figure 7; Table D2). Less mobile deposit-feeders, such as *Scoloplos armiger* and highly mobile suspension feeders like *Ensis leei* (Kranz, 1974; Shumway et al., 1985), showed high occurrence rates at intermediate TRI (weighted average of 3.94 for both) (Fig. 6) where they are able to outmove burial. Moreover, *S. armiger* and *E. leei*, both show an ecological optimum for TRI (binomial regression, B_{TRI} = 2.46, 95% CI = [1.31, 3.62], B_{TRI}^2 = −0.31, 95% CI = [−0.45, −0.18] and B_{TRI} = 1.90, 95% CI = [0.71, 3.12], B_{TRI}^2 = −0.24, 95% CI = [−0.39, −0.10], respectively; Figure 7; Table D2). Sedentary deposit-feeders like *Aphelochaeta marioni* (Bolam, 2011), suspension feeders like *Mya arenaria* (Kranz, 1974) and *Cerastoderma edule* (André & Rosenberg, 1991) are very sensitive to burial (Bolam, 2011), hence their association with low TRI (Fig. 6). *C. edule* and
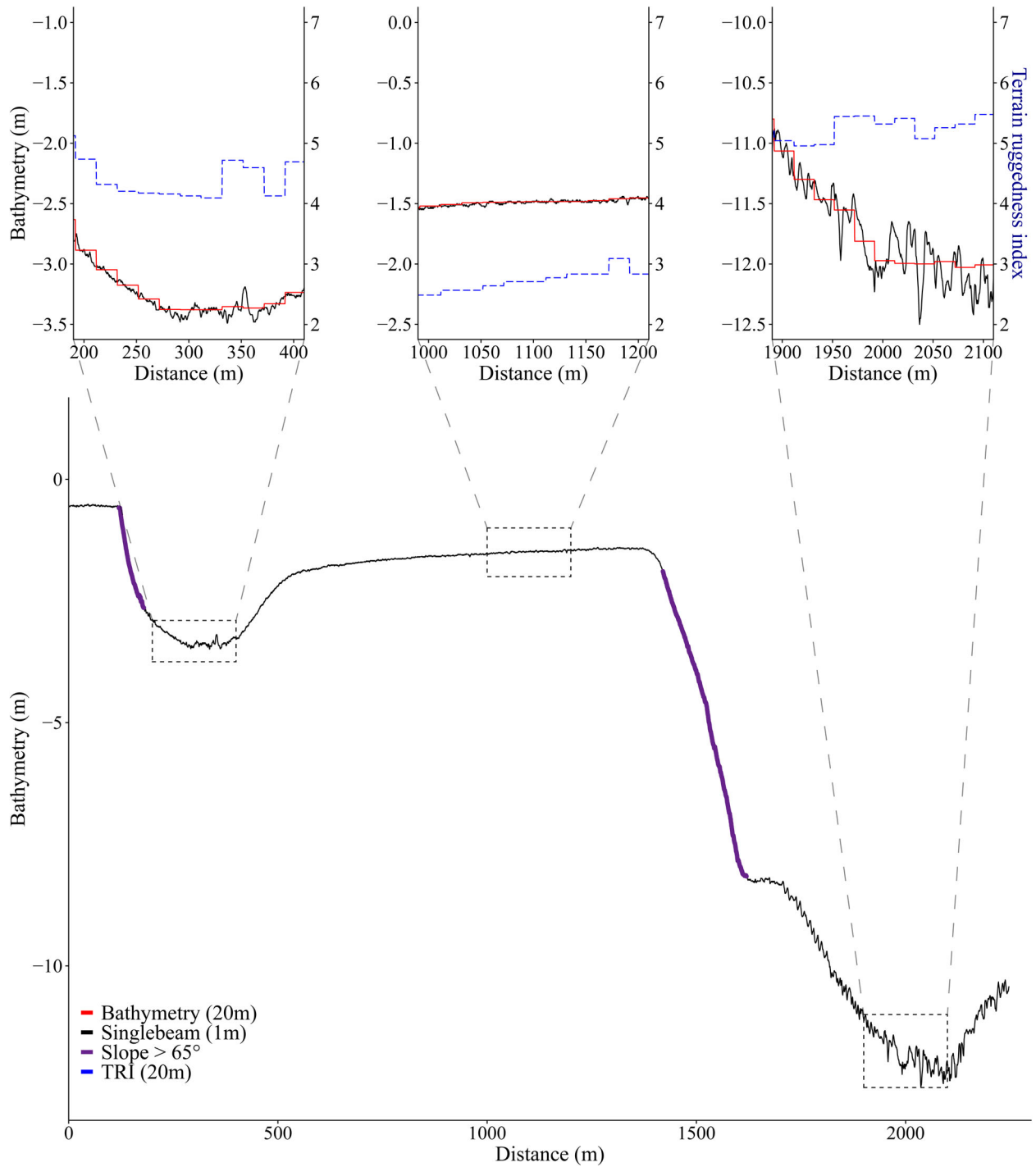
Figure 4. Raw single-beam transect data of the 1-meter resolution bathymetry and zoomed in areas with corresponding TRI values on a 20-meter resolution (blue dashed lines) of intermediate, high and low bathymetry respectively from left to right. The red line depicts the 20-meter interpolated bathymetry, and the dark purple lines reflect the mask from slopes higher than 65 degrees. The transect runs from south to north and is indicated by a red arrow in Figure 2.

Peringia ulvae are both associated with the lowest weighted average of TRI of 3.06 and 3.13, respectively and show decreasing occurrence with increasing TRI (binomial regression, $B = -1.00$, 95% CI $= [-1.36, -0.60]$ and $B = -0.87$, 95% CI $= [-1.23, -0.56]$, respectively; Figure 7; Table D2).
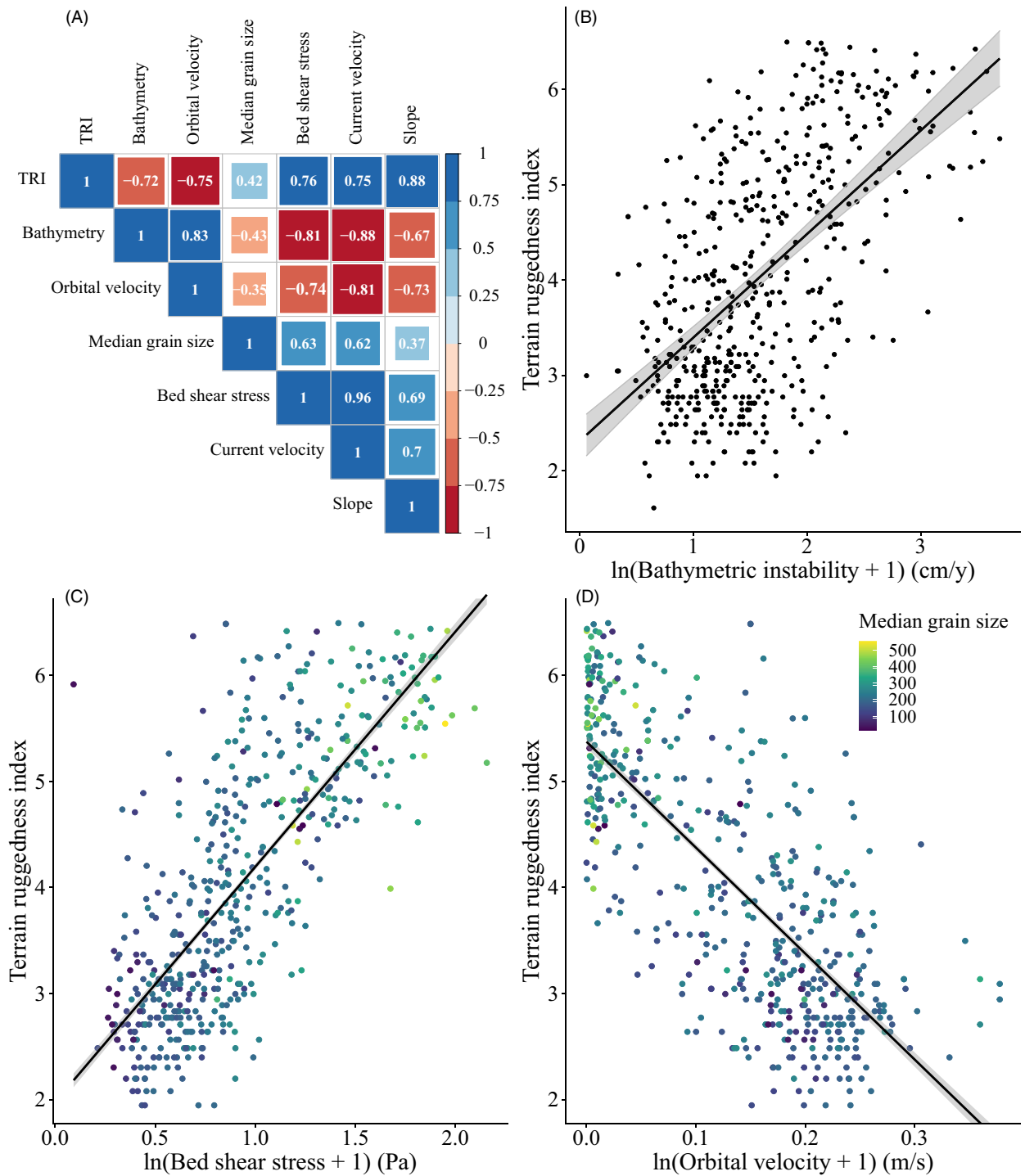
Figure 5. (A) Correlogram of significant Pearson correlation coefficients between TRI and all hydrodynamic and bathymetric factors. Color scale represents strength of the correlation with red being strongly negatively correlated and blue strongly positively correlated. Relationship between Terrain ruggedness index and abiotic factors: (B) ln(x + 1) transformed bathymetric instability (cm/y); (C) orbital velocity; and (D) bed shear stress. 95% Confidence intervals are depicted in gray. Color gradient depicts median grain size ranging from low in blue to high in yellow.
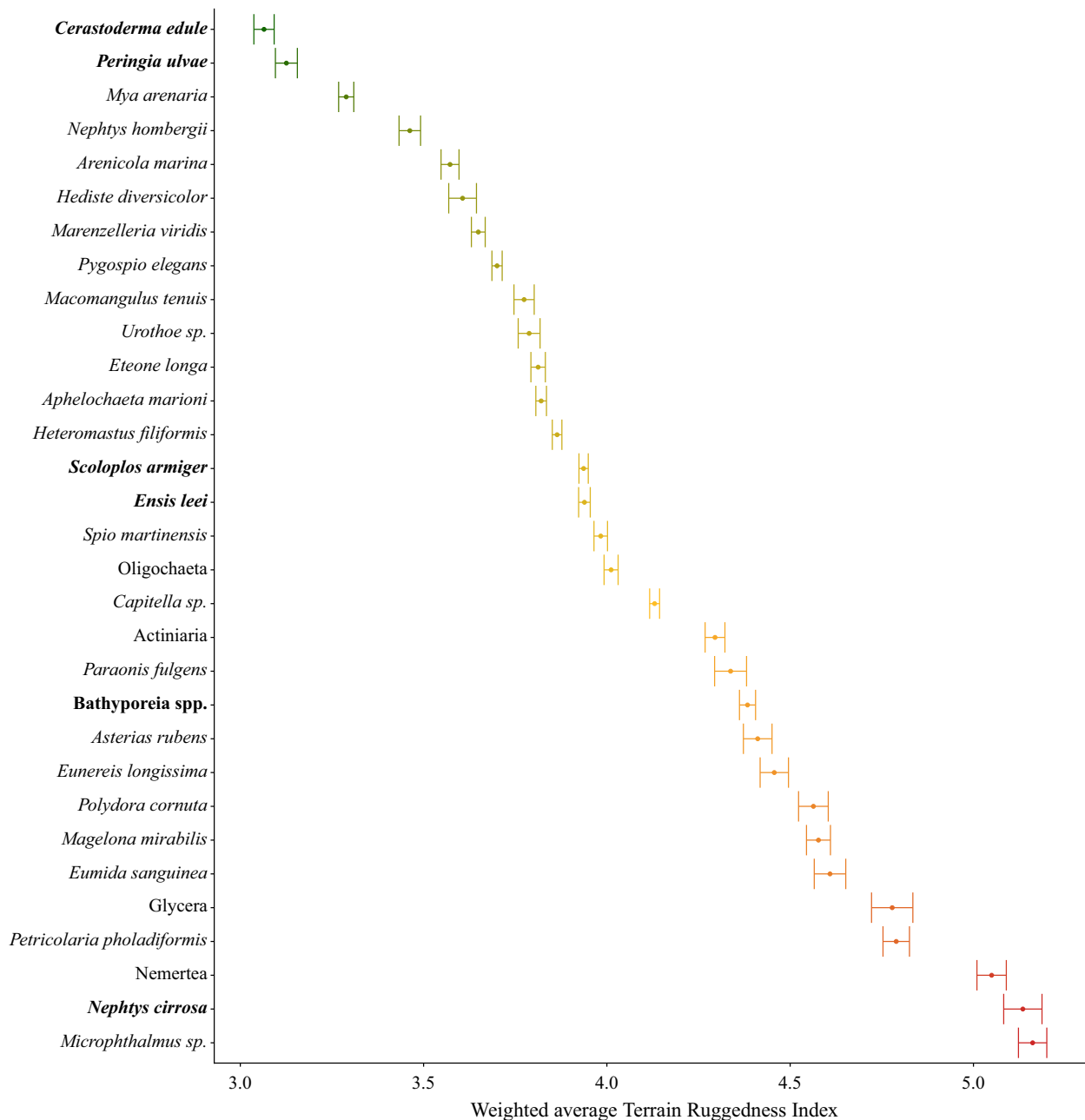
Figure 6. Weighted average of Terrain Ruggedness Index per species. Bars represent standard error. Color gradient depicts TRI values with low values in green and high values in red. Highlighted species were further analyzed using logistic regression (Fig. 7).

Discussion

We have outlined in this paper a novel method to determine fine-scale seabed morphology using existing single-beam echosounding data which can be used to predict macrozoobenthic species occurrence. We find that Terrain Ruggedness Index (TRI) accurately captures small-scale bathymetric variation. Variation in TRI related to both spatial and temporal dynamics of the seafloor and was found to be highly correlated with bed shear stress and orbital velocity. In addition, TRI significantly predicted the occurrence of 31 out of 50 macrozoobenthic taxa that were found in a large-scale sampling campaign. We indeed observed a trophic shift from sedentary deposit-feeders and suspension feeders in low dynamic (indicated by low TRI) areas to mobile scavenger–predator and mobile deposit-feeding macrozoobenthic species in highly dynamic (indicated by high TRI) areas.
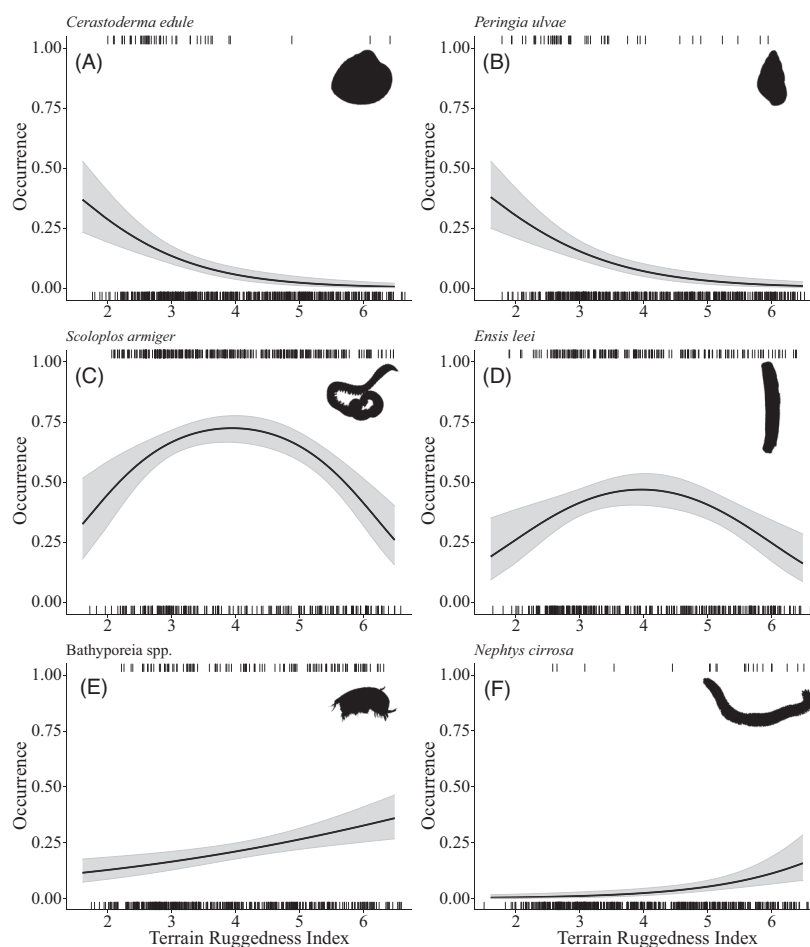
Figure 7. Relationship between Terrain Ruggedness Index and occurrence of several species: (A) *Cerastoderma edule*; (B) *Peringia ulvae*; (C) *Scoloplos armiger*; (D) *Ensis leei*; (E) *Bathyporeia* spp.; and (F) *Nephtys cirrosa*. 95% Confidence intervals are depicted in gray. Ticks at the top and the bottom of the y-axis represent the presence and absence of each species.

Dynamic areas with high burial rates, such as megaripple areas characterized by high TRI, are expected to be dominated by species with short lifespans and fast reproduction (Holzhauer et al., 2022), mobile predator–scavengers or deposit-feeders (Robert et al., 2021; van der Wal, Ysebaert, et al., 2017b). Detailed occurrence, dynamics and biotic relationships of multiscale bedforms have been studied extensively by multibeam echosounding for a smaller part of the Dutch Wadden Sea, the ebb-tidal delta of the Ameland inlet (*e.g.* Brakenhoff, 2021; Holzhauer et al., 2019, 2022; van Prooijen et al., 2020). Holzhauer et al. (2022) highlight strong responses of the benthic community to morphometric seabed properties. However, high-resolution mapping of shallow soft-bottom systems, such as the Dutch Wadden Sea, to characterize these morphometric seabed properties was not done due to the complications of using multibeam sonar in shallow seas. We show that the TRI we have calculated using existing single-beam data is a good indicator of morphometric seabed properties such as megaripples. Comparing the calculated TRI values to single-beam transects shows clear patterns between TRI and bathymetric variations. Small bathymetric variation, indicating smaller megaripples, found in the shallower gullies under influence of intermediate hydrodynamic forcing, is associated with intermediate TRI values ranging from 4 to 5. Shallow sand flats, with lower hydrodynamic forcing through bed shear stress, show less bathymetric variation, and hence are associated with low TRI values (<4). Contrastingly, deeper gullies that are known for their rough hydrodynamic conditions show the largest variations in bathymetry and similarly have highest TRI values (>5). Despite the fact that the single-beam transects do not line up crossing megaripple formations, we are still able to discern these bedform formations and the strength of their formation. Prior knowledge of the general direction of megaripples (*e.g.* by adding high-resolution single-beam transects in the direction of flow) would enable

more accurate mapping of their effects as well as give information of their specific morphometrics (*i.e.* wave length, migration speed). Still, by taking a larger window size when calculating TRI, we ensure the inclusion of at least one crest and trough to be able to identify the presence of megaripple formation and gauge the strength of their migration. Areas with high TRI and thus largest bathymetric variation are then hypothesized to have the largest sediment displacement. Species in these areas have to be adapted to constant burial by large amounts of sediment. They need to be highly mobile and resilient enough to withstand constant disturbance, as confirmed by our results.

Using historical bathymetric data, we found that spatial heterogeneity of the seafloor as measured by TRI is a good indicator for its larger scale temporal bathymetric instability with large potential implication for macrozoobenthic species distributions. These dynamics are largely driven by the interplay between sediment and hydrodynamic conditions, such as bed shear stress and orbital velocity. The intensity of hydrodynamic forcing affects rates of sedimentation and erosion, so natural dynamics of seafloor habitats, with largest ecological impacts are expected at intermediate forcing (Fig. 1). Here, we found high TRI to be indicative of high dynamic areas as high TRI was strongly related to hydrodynamic forcing (*i.e.*, bed shear stress and orbital velocity). As this relationship was log-linear, the untransformed fitted models show an exponential increase of TRI (and thus seabed dynamics) with higher bed shear stress. However, it can be argued that with even higher hydrodynamic forcing the system would shift from soft-bottom to hard substrate with only rocks being able to remain. Consequently, bedform dynamics would get lost and thus only able to be sustained at intermediate hydrodynamic forcing. High TRI was also related to high temporal bathymetric instability. High temporal instability indicates large and fast movement of sediment, resulting in large annual differences in depth through the constant migration of bedforms. The strong relationship between the spatial heterogeneity captured by TRI and the temporal variability in bathymetry emphasizes the quality of TRI as an indicator of ecologically relevant bedforms, such as megaripples. High TRI values thus reflect the massive sediment transport and constant burial that species have to deal with. This imposes a strong selection for species that are highly mobile either through the water- and/or sediment column (Hinchey et al., 2006; van der Wal, Ysebaert, et al., 2017b; Zühlke & Reise, 1994).

The physical forces imposed by hydrodynamics and related migrating bedforms, as captured by the TRI, is expected to be reflected in the functional trait makeup of a macrozoobenthic community. We find sedentary deposit-feeders and suspension feeders like *Aphelochaeta marioni* (Bolam, 2011), *Mya arenaria* (Kranz, 1974) and *Cerastoderma edule* (André & Rosenberg, 1991) in low TRI areas, whereas high TRI areas are characterized by mobile deposit-feeders and scavenger-–predators like *Bathyporeia* spp. (Fauchald, 1977; Nicolaisen & Kanneworff, 1969), *Nephtys cirrosa* and *Eumida sanguinea* (Fauchald, 1977; Hayward & Ryland, 2017). Other studies on macrozoobenthic communities in response to natural dynamics find similar results. van der Wal, Lambert, et al. (2017a) found a trophic shift from a deposit-feeding community (*e.g.*, *Heteromastus filiformis*, *Scoloplos armiger* and *A. marioni*) in low hydrodynamic conditions to a predator and omnivore-dominated community with high mobility (*e.g.*, *Nephtys* spp.) in the Westerschelde estuary. Highly dynamic areas in the ebb-tidal delta of the Ameland inlet were characterized by *B. pelagica*, *B. elegans* and *N. cirrosa* (Holzhauer et al., 2022). Contrastingly, species like *Urothoe poseidonis* and *Nephtys hombergii* were indicative of low dynamic areas (Holzhauer et al., 2022). Likewise, van der Wal, Ysebaert, et al. (2017b) found high energetic sites with large bathymetric variation to be distinguished by *Bathyporeia* spp. and *Nephtys* spp., whereas *H. filiformis* and *S. armiger* were mainly found in low-to-intermediate energetic sites. *Pygospio elegans* and *Hediste diversicolor* were especially indicative of low-to-intermediate energetic sites (van der Wal, Ysebaert, et al., 2017b). The high degree of similarities between bedform-species patterns observed in previous studies and this study using TRI, further indicates the potential to use this proxy for large-scale bedform characterization for habitat modeling.

Seafloor morphodynamics not only predicts species occurrence, but is also subject to dominant macrobenthic species that influence sediment dynamics. Interactions between the bioturbating activities, or the presence of ecosystem engineers might alter the formation of bedform patterns (*e.g.* Borsje et al., 2009; Damveld et al., 2020; Malarkey et al., 2015), and thereby provide protection from hydrodynamics and facilitate more sensitive species. Van der Reijden et al. (2021) found patches of *Sabellaria spinulosa*, an epibenthic reef-forming polychaete, in the troughs of megaripple waves in the North Sea. They hypothesized the *S. spinulosa* reefs to be capable of reducing megaripple migration to rates these reefs can cope with (van der Reijden et al., 2021). Modeling studies show the two-way coupling of *Lanice conchilega* reefs and sand wave morphology (Damveld et al., 2019, 2020). Hydrodynamic attenuation of other reef-forming species might also influence the formation of bedform structures. Blue mussel (*Mytilus edulis*) beds are known to greatly influence near-bed flow properties (Folkard & Gascoigne, 2009; van Leeuwen et al., 2010). This may alter

bedform formation and migration and facilitate more sensitive species in otherwise high dynamic areas. Discrepancies in TRI and hydrodynamics might be due to the presence of biogenic reefs. Unfortunately, our sampling method was too coarse to properly assess the spatial extent of biogenic reefs to make this comparison. Additionally, boxcoring is not a suitable method to sample hard substrates like bivalve beds as the core will not penetrate the reef. This may have caused an underrepresentation of species in bivalve beds. Nevertheless, low TRI values in areas despite strong hydrodynamic conditions might then hint at the occurrence of sediment stabilizing species and warrant further inspection as these areas might be of high natural value.

Additional anthropogenic disturbances within highly dynamic areas are usually considered negligible (Bergman et al., 2015; Rijnsdorp et al., 2018), but this has been poorly tested until now for shallow coastal waters. Hydrodynamic conditions can shape macrozoobenthic communities along gradients of resistance to physical disturbances (Hershkovitz & Gasith, 2013; van der Wal, Lambert, et al., 2017a; Warwick & Uncles, 1980). High physical forcing in dynamic areas then predispose macrozoobenthic communities to be resistant against additional anthropogenic perturbations (Rijnsdorp et al., 2018). Alternatively, a long history of continued anthropogenic disturbance may have altered benthic communities to be predisposed to withstand disturbances, regardless of their natural dynamics (Bergman et al., 2015). In addition, highly energetic hydrodynamic conditions in soft-bottom systems can give rise to sand wave structures (Passchier & Kleinhans, 2005). These bedforms in turn alter hydrodynamic conditions, creating microclimates with calmer conditions that allow more sensitive species to persist (Hoziaux et al., 2008; Mestdagh et al., 2020; van der Reijden et al., 2019). These communities might then not be able to persist under high anthropogenic pressures. Still, bedform structures such as megaripples are often superimposed on larger bedforms such as sand waves (Koop & Amiri-Simkooei, 2019; Lindenbergh et al., 2006), adding to the spatial complexity of species responses to hydrodynamic conditions as well as their resistance to additional anthropogenic perturbations. Characterizing all natural physical forces allows for the appropriate incorporation of the natural dynamics background when studying the impact of anthropogenic disturbances on ecosystem functioning and biodiversity in shallow coastal ecosystems.

Conclusion

High-resolution marine habitat mapping can not only help in understanding species distributions but also in prioritizing conservation areas by identifying areas with the potential to develop or sustain communities of sensitive species. Here, we have shown a method to repurpose existing single-beam data to map seafloor dynamics on a large spatial scale. By repurposing the data of an existing program there is no need for additional mapping programs that are usually expensive and often logistically challenging. The strong correlation with hydrodynamics highlights TRI as an indicator for natural dynamics and can help in discerning the effects of natural- and anthropogenic dynamics in relation to questions about the impact of anthropogenic activities such as bottom trawling. The obtained information can then be used for conservation and marine spatial planning purposes. Integrating measures of natural dynamics in marine spatial planning and the decisions for placing Marine Protected Areas will aid in a sustainable division of seafloor habitats between nature conservation and anthropogenic use.

Acknowledgments

References

Alin, A. (2010) Multicollinearity. *WIREs Computational Statistics*, **2**(3), 370–374. https://doi.org/10.1002/wics.84

André, C. & Rosenberg, R. (1991) Adult-larval interactions in the suspension-feeding bivalves Cerastoderma edule and Mya arenaria. *Marine Ecology Progress Series*, **71**, 227–234. https://doi.org/10.3354/meps071227

Baptist, M.J., van Dalfsen, J., Weber, A., Passchier, S. & van Heteren, S. (2006) The distribution of macrozoobenthos in the southern North Sea in relation to meso-scale bedforms. *Estuarine, Coastal and Shelf Science*, **68**(3), 538–546. https://doi.org/10.1016/j.ecss.2006.02.023

Barbier, E.B., Hacker, S.D., Kennedy, C., Koch, E.W., Stier, A.C. & Silliman, B.R. (2011) The value of estuarine and coastal ecosystem services. *Ecological Monographs*, **81**(2), 169–193. https://doi.org/10.1890/10-1510.1

Barman, N.K., Chatterjee, S. & Paul, A.K. (2016) Materials and methods: a framework for the coastal morphodynamics. In: Barman, N.K., Chatterjee, S. & Paul, A.K. (Eds.) *Coastal*

morphodynamics, Cham: Springer International Publishing, pp. 17–46. https://doi.org/10.1007/978-3-319-33575-9_3

Barnard, P.L., Erikson, L.H. & Kvitek, R.G. (2011) Small-scale sediment transport patterns and bedform morphodynamics: new insights from high-resolution multibeam bathymetry. *Geo-Marine Letters*, **31**(4), 227–236. https://doi.org/10.1007/s00367-011-0227-1

Bergman, M.J.N., Ubels, S.M., Duineveld, G.C.A. & Meesters, E.W.G. (2015) Effects of a 5-year trawling ban on the local benthic community in a wind farm in the Dutch coastal zone. *ICES Journal of Marine Science*, **72**(3), 962–972. https://doi.org/10.1093/icesjms/fsu193

Bolam, S.G. (2011) Burial survival of benthic macrofauna following deposition of simulated dredged material. *Environmental Monitoring and Assessment*, **181**(1), 13–27. https://doi.org/10.1007/s10661-010-1809-5

Borsje, B.W., de Vries, M.B., Bouma, T.J., Besio, G., Hulscher, S.J.M.H. & Herman, P.M.J. (2009) Modeling bio-geomorphological influences for offshore sandwaves. *Continental Shelf Research*, **29**(9), 1289–1301. https://doi.org/10.1016/j.csr.2009.02.008

Brakenhoff, L.B. (2021) *Bedforms and their effect on sediment transport on ebb-tidal deltas*. Utrecht: Utrecht University. https://doi.org/10.33540/588

Compton, T.J., Holthuijsen, S., Koolhaas, A., Dekinga, A., ten Horn, J., Smith, J. et al. (2013) Distinctly variable mudscapes: distribution gradients of intertidal macrofauna across the Dutch Wadden Sea. *Journal of Sea Research*, **82**, 103–116. https://doi.org/10.1016/j.seares.2013.02.002

Costanza, R., d'Arge, R., de Groot, R., Farber, S., Grasso, M., Hannon, B. et al. (1997) The value of the world's ecosystem services and natural capital. *Nature*, **387**(6630), 253–260. https://doi.org/10.1038/387253a0

Damveld, J.H., Borsje, B.W., Roos, P.C. & Hulscher, S.J.M.H. (2020) Biogeomorphology in the marine landscape: modelling the feedbacks between patches of the polychaete worm Lanice conchilega and tidal sand waves. *Earth Surface Processes and Landforms*, **45**(11), 2572–2587. https://doi.org/10.1002/esp.4914

Damveld, J.H., Roos, P.C., Borsje, B.W. & Hulscher, S.J.M.H. (2019) Modelling the two-way coupling of tidal sand waves and benthic organisms: a linear stability approach. *Environmental Fluid Mechanics*, **19**(5), 1073–1103. https://doi.org/10.1007/s10652-019-09673-1

Damveld, J.H., van der Reijden, K.J., Cheng, C., Koop, L., Haaksma, L.R., Walsh, C.A.J. et al. (2018) Video transects reveal that tidal sand waves affect the spatial distribution of benthic organisms and sand ripples. *Geophysical Research Letters*, **45**(21), 11,837–11,846. https://doi.org/10.1029/2018GL079858

de Jong, M.F., Baptist, M.J., Lindeboom, H.J. & Hoekstra, P. (2015) Relationships between macrozoobenthos and habitat characteristics in an intensively used area of the Dutch coastal zone. *ICES Journal of Marine Science*, **72**(8), 2409–2422. https://doi.org/10.1093/icesjms/fsv060

de Kruif, A. C. (2001). *Bodemdieptegegevens van het Nederlandse Kustsysteem (RIKZ/2001.041; p. 114)*. Utrecht: Rijkswaterstaat.

Dodd, N., Blondeaux, P., Calvete, D., Swart, H.E.D. & Falques, A. (2003) Understanding coastal morphodynamics using stability methods. *Journal of Coastal Research*, **19**(4), 18.

Elias, E. (2006) *Morphodynamics of Texel inlet*. Amsterdam: IOS Press.

Ernstsen, V.B., Noormets, R., Winter, C., Hebbeln, D., Bartholomä, A., Flemming, B.W. et al. (2005) Development of subaqueous barchanoid-shaped dunes due to lateral grain size variability in a tidal inlet channel of the Danish Wadden Sea. *Journal of Geophysical Research: Earth Surface*, **110**(F4), F04S08. https://doi.org/10.1029/2004JF000180

Evans, J. S., Murphy, M. A., & Ram, K. (2021). *SpatialEco (1.3-7). [Computer software]*. https://github.com/jeffreyevans/spatialEco

Fauchald, K. (1977) *The polychaete worms. Definitions and keys to the orders, families and genera*. Los Angeles: Natural History Museum of Los Angeles County.

Flemming, B.W. (1988) Zur Klassifikation subaquatischer, strömungstransversaler Transportkörper. *Bochumer geologische und geotechnische Arbeiten*, **29**, 44–47.

Folkard, A.M. & Gascoigne, J.C. (2009) Hydrodynamics of discontinuous mussel beds: laboratory flume simulations. *Journal of Sea Research*, **62**(4), 250–257. https://doi.org/10.1016/j.seares.2009.06.001

Franken, O., Holthuijsen, S., Meijer, K. J., Kleine Schaars, L., Rasch, B., Kooiman, J., et al. (n.d.). Below murky waters: large spatial sampling campaign of the subtidal Dutch Wadden Sea elucidates sediment composition and dominant species distributions. In Prep.

Harley, C.D.G., Randall Hughes, A., Hultgren, K.M., Miner, B.G., Sorte, C.J.B., Thornber, C.S. et al. (2006) The impacts of climate change in coastal marine systems. *Ecology Letters*, **9**(2), 228–241. https://doi.org/10.1111/j.1461-0248.2005.00871.x

Hayward, P.J. & Ryland, J.S. (Eds.). (2017) *Handbook of the marine Fauna of North-West Europe*. Oxford: Oxford University Press. https://doi.org/10.1093/acprof:oso/9780199549443.001.0001

He, Q. & Silliman, B.R. (2019) Climate change, human impacts, and coastal ecosystems in the Anthropocene. *Current Biology*, **29**(19), R1021–R1035. https://doi.org/10.1016/j.cub.2019.08.042

Hershkovitz, Y. & Gasith, A. (2013) Resistance, resilience, and community dynamics in mediterranean-climate streams. *Hydrobiologia*, **719**(1), 59–75. https://doi.org/10.1007/s10750-012-1387-3

Hinchey, E.K., Schaffner, L.C., Hoar, C.C., Vogt, B.W. & Batte, L.P. (2006) Responses of estuarine benthic invertebrates to sediment burial: the importance of mobility and adaptation. *Hydrobiologia*, **556**(1), 85–98. https://doi.org/10.1007/s10750-005-1029-0

Holzhauer, H., Borsje, B.W., Herman, P.M.J., Schipper, C.A. & Wijnberg, K.M. (2022) The geomorphology of an ebb-tidal-delta linked to benthic species distribution and functionality. *Ocean and Coastal Management*, **216**, 105938. https://doi.org/10.1016/j.ocecoaman.2021.105938

Holzhauer, H., Borsje, B.W., van Dalfsen, J.A., Wijnberg, K.M., Hulscher, S.J.M.H. & Herman, P.M.J. (2019) Benthic species distribution linked to morphological features of a barred coast. *Journal of Marine Science and Engineering*, **8**(1), 16. https://doi.org/10.3390/jmse8010016

Hoziaux, J.S., Kerckhof, F., Degrendele, K., Roche, M. & Norro, A. (2008) *The hinder banks: yet an important region for the Belgian marine biodiversity?*. Brussels: Belgian Science Policy. http://www.belspo.be/belspo/organisation/publ/pub_ostc/EV/rappEV45_en.pdf

Hulscher, S.J.M.H. (1996) Tidal-induced large-scale regular bed form patterns in a three-dimensional shallow water model. *Journal of Geophysical Research: Oceans*, **101**(C9), 20727–20744. https://doi.org/10.1029/96JC01662

Idier, D., Astruc, D. & Hulscher, S.J.M.H. (2004) Influence of bed roughness on dune and megaripple generation. *Geophysical Research Letters*, **31**(13), L13214. https://doi.org/10.1029/2004GL019969

Kassambara, A. (2019). *ggcorrplot: Visualization of a Correlation Matrix using "ggplot2"* (R package version 0.1.3) [Computer software]. https://CRAN.R-project.org/package=ggcorrplot

Knaapen, M.a.F. (2005) Sandwave migration predictor based on shape information. *Journal of Geophysical Research: Earth Surface*, **110**(F4), F04S11. https://doi.org/10.1029/2004JF000195

Koop, L., Amiri-Simkooei, A.J., van der Reijden, K., O'Flynn, S., Snellen, M.G. & Simons, D. (2019) Seafloor classification in a sand wave environment on the Dutch continental shelf using multibeam echosounder backscatter data. *Geosciences*, **9**(3), 142.

Kraft, N.J.B., Adler, P.B., Godoy, O., James, E.C., Fuller, S. & Levine, J.M. (2015) Community assembly, coexistence and the environmental filtering metaphor. *Functional Ecology*, **29**(5), 592–599. https://doi.org/10.1111/1365-2435.12345

Kranz, P.M. (1974) The Anastrophic burial of bivalves and its paleoecological significance. *The Journal of Geology*, **82**(2), 237–265. https://doi.org/10.1086/627961

Landero Figueroa, M.M., Parsons, M.J.G., Saunders, B.J., Radford, B., Salgado-Kent, C. & Parnum, I.M. (2021) The use of singlebeam echo-sounder depth data to produce demersal fish distribution models that are comparable to models produced using multibeam echo-sounder depth. *Ecology and Evolution*, **11**(24), 17873–17884. https://doi.org/10.1002/ece3.8351

Lefebvre, A., Paarlberg, A.J. & Winter, C. (2016) Characterising natural bedform morphology and its influence on flow. *Geo-Marine Letters*, **36**(5), 379–393. https://doi.org/10.1007/s00367-016-0455-5

Lindenbergh, R.C., van Dijk, T.A.G.P. & Egberts, P.J.P. (2006) Separating bedforms of different scales in Echo sounding data. *Coastal Dynamics*, **2005**, 1–14. https://doi.org/10.1061/40855(214)6

Lotze, H.K., Reise, K., Worm, B., van Beusekom, J., Busch, M., Ehlers, A. et al. (2005) Human transformations of the Wadden Sea ecosystem through time: a synthesis. *Helgoland Marine Research*, **59**(1), 84–95. https://doi.org/10.1007/s10152-004-0209-z

Malarkey, J., Baas, J.H., Hope, J.A., Aspden, R.J., Parsons, D.R., Peakall, J. et al. (2015) The pervasive role of biological cohesion in bedform development. *Nature Communications*, **6**(1), 6257. https://doi.org/10.1038/ncomms7257

Markert, E., Kröncke, I. & Kubicki, A. (2015) Small scale morphodynamics of shoreface-connected ridges and their impact on benthic macrofauna. *Journal of Sea Research*, **99**, 47–55. https://doi.org/10.1016/j.seares.2015.02.001

Mestdagh, S., Amiri-Simkooei, A., van der Reijden, K.J., Koop, L., O'Flynn, S., Snellen, M. et al. (2020) Linking the morphology and ecology of subtidal soft-bottom marine benthic habitats: a novel multiscale approach. *Estuarine, Coastal and Shelf Science*, **238**(106687), 11. https://doi.org/10.1016/j.ecss.2020.106687

Morales, J.A., Delgado, I. & Mas, J.M.G. (2015) Bedform variability and flow regime in a barrier-inlet system. The mesotidal Piedras mouth (Huelva, SW Spain). *Geologica Acta*, **13**(2), 137–153.

Nicolaisen, W. & Kanneworff, E. (1969) On the burrowing and feeding habits of the amphipods Bathyporeia pilosa Lindström and Bathyporeia sarsi Watkin. *Ophelia*, **6**(1), 231–250. https://doi.org/10.1080/00785326.1969.10409651

Oost, A., Cleveringa, J. & Taal, M. (2018) *Morfologie Kombergingsgebieden Marsdiep en Vlie* (No. 11202177–000; p. 99). Delft: Deltares.

Passchier, S. & Kleinhans, M.G. (2005) Observations of sand waves, megaripples, and hummocks in the Dutch coastal area and their relation to currents and combined flow conditions. *Journal of Geophysical Research: Earth Surface*, **110**(F4), F04S15. https://doi.org/10.1029/2004JF000215

Pitcher, C.R., Hiddink, J.G., Jennings, S., Collie, J., Parma, A.M., Amoroso, R. et al. (2022) Trawl impacts on the relative status of biotic communities of seabed sedimentary habitats in 24 regions worldwide. *Proceedings of the National Academy of Sciences*, **119**(2), e2109449119. https://doi.org/10.1073/pnas.2109449119

QGIS Development Team. (2021). *QGIS geographic information system* (3.18.1) [Computer software].

R Core Team. (2021). *R: a language and environment for statistical computing*. R foundation for statistical computing. Vienna: R Foundation for Statistical Computing. https://www.R-project.org/

Reise, K. (2005) Coast of change: habitat loss and transformations in the Wadden Sea. *Helgoland Marine Research*, **59**(1), 9–21. https://doi.org/10.1007/s10152-004-0202-6

Rijkswaterstaat, RIKZ. (2021). *MARIA* (9.46) [Computer software]. Culemborg: Modelit.

Rijnsdorp, A.D., Bolam, S.G., Garcia, C., Hiddink, J.G., Hintzen, N.T., van Denderen, P.D. et al. (2018) Estimating sensitivity of seabed habitats to disturbance by bottom trawling based on the longevity of benthic fauna. *Ecological Applications*, 28(5), 1302–1312. https://doi.org/10.1002/eap.1731

Rippen, A., van der Zee, E., Fieten, N., Latour, J. & Wymenga, E. (2021) *Review effecten natuurlijke bodemdynamiek en menselijke bodemberoering in de sublitorale Waddenzee.* Veenwouden: Altenburg & Wymenga.

Robert, A.E., Quillien, N., Bacha, M., Caulle, C., Nexer, M., Parent, B. et al. (2021) Sediment migrations drive the dynamic of macrobenthic ecosystems in subtidal sandy bedforms. *Marine Pollution Bulletin*, 171, 112695. https://doi.org/10.1016/j.marpolbul.2021.112695

Rosenberg, R. (1995) Benthic marine fauna structured by hydrodynamic processes and food availability. *Netherlands Journal of Sea Research*, 34(4), 303–317. https://doi.org/10.1016/0077-7579(95)90040-3

Shumway, S.E., Cucci, T.L., Newell, R.C. & Yentsch, C.M. (1985) Particle selection, ingestion, and absorption in filter-feeding bivalves. *Journal of Experimental Marine Biology and Ecology*, 91(1–2), 77–92. https://doi.org/10.1016/0022-0981(85)90222-9

Snelgrove, P.V.R. (1999) Getting to the bottom of marine biodiversity: sedimentary habitats: ocean bottoms are the most widespread habitat on earth and support high biodiversity and key ecosystem services. *Bioscience*, 49(2), 129–138. https://doi.org/10.2307/1313538

Ter Braak, C.J.F. & Prentice, I.C. (2004) A theory of gradient analysis. In: Caswell H. (Ed.) *Advances in ecological research*, Cambridge: Elsevier, Vol. 34, pp. 235–282. https://doi.org/10.1016/S0065-2504(03)34003-6

van Dalfsen, J.A., Essink, K., Madsen, H.T., Birklund, J., Romero, J. & Manzanera, M. (2000) Differential response of macrozoobenthos to marine sand extraction in the North Sea and the Western Mediterranean. *ICES Journal of Marine Science*, 57(5), 1439–1445. https://doi.org/10.1006/jmsc.2000.0919

van der Reijden, K.J., Koop, L., Mestdagh, S., Snellen, M., Herman, P.M.J., Olff, H. et al. (2021) Conservation implications of Sabellaria spinulosa reef patches in a dynamic Sandy-bottom environment. *Frontiers in Marine Science*, 8, 642659. https://doi.org/10.3389/fmars.2021.642659

van der Reijden, K.J., Koop, L., O'Flynn, S., Garcia, S., Bos, O., van Sluis, C. et al. (2019) Discovery of Sabellaria spinulosa reefs in an intensively fished area of the Dutch continental shelf, North Sea. *Journal of Sea Research*, 144, 85–94. https://doi.org/10.1016/j.seares.2018.11.008

van der Wal, D., Lambert, G.I., Ysebaert, T., Plancke, Y.M.G. & Herman, P.M.J. (2017a) Hydrodynamic conditioning of diversity and functional traits in subtidal estuarine macrozoobenthic communities. *Estuarine, Coastal and Shelf Science*, 197, 80–92. https://doi.org/10.1016/j.ecss.2017.08.012

van der Wal, D., Ysebaert, T. & Herman, P.M.J. (2017b) Response of intertidal benthic macrofauna to migrating megaripples and hydrodynamics. *Marine Ecology Progress Series*, 585, 17–30. https://doi.org/10.3354/meps12374

van Leeuwen, B., Augustijn, D.C.M., van Wesenbeeck, B.K., Hulscher, S.J.M.H. & de Vries, M.B. (2010) Modeling the influence of a young mussel bed on fine sediment dynamics on an intertidal flat in the Wadden Sea. *Ecological Engineering*, 36(2), 145–153. https://doi.org/10.1016/j.ecoleng.2009.01.002

van Prooijen, B.C., Tissier, M.F.S., de Wit, F.P., Pearson, S.G., Brakenhoff, L.B., van Maarseveen, M.C.G. et al. (2020) Measurements of hydrodynamics, sediment, morphology and benthos on Ameland ebb-tidal delta and lower shoreface. *Earth System Science Data*, 12(4), 2775–2786. https://doi.org/10.5194/essd-12-2775-2020

Van Weerdenburg, R. & Vroom, J. (2021) *Model parameters Ecotopenkaart Waddenzee* (No. 11206799-003-ZKS-0003). Delft: Deltares.

Wang, Z.B., Hoekstra, P., Burchard, H., Ridderinkhof, H., De Swart, H.E. & Stive, M.J.F. (2012) Morphodynamics of the Wadden Sea and its barrier Island system. *Ocean and Coastal Management*, 68, 39–57. https://doi.org/10.1016/j.ocecoaman.2011.12.022

Warwick, R. & Uncles, R. (1980) Distribution of benthic macrofauna associations in the Bristol Channel in relation to tidal stress. *Marine Ecology Progress Series*, 3, 97–103. https://doi.org/10.3354/meps003097

Wever, T. (2004) Bedforms and bedform migration: a data review. In: Hulscher, S.J.M.H., Garlan, T.E. & Idier, D. (Eds). *Proc. Marine and River Dune Dynamics*, Enschede: University of Twente, pp. 330–337.

Wilson, M.F.J., O'Connell, B., Brown, C., Guinan, J.C. & Grehan, A.J. (2007) Multiscale terrain analysis of multibeam bathymetry data for habitat mapping on the continental slope. *Marine Geodesy*, 30(1–2), 3–35. https://doi.org/10.1080/01490410701295962

Wood, S.N. (2011) Fast stable restricted maximum likelihood and marginal likelihood estimation of semiparametric generalized linear models. *Journal of the Royal Statistical Society: Series B (Statistical Methodology)*, 73(1), 3–36. https://doi.org/10.1111/j.1467-9868.2010.00749.x

Zühlke, R. & Reise, K. (1994) Response of macrofauna to drifting tidal sediments. *Helgoländer Meeresuntersuchungen*, 48(2), 277–289. https://doi.org/10.1007/BF02367041

Supporting Information

Additional supporting information may be found online in the Supporting Information section at the end of the article.

Appendix S1. Comparison of singlebeam transect direction.